Biogeochemistry (2012) 107:319–338
DOI 10.1007/s10533-010-9555-x

# Three-dimensional spatial patterns of trace gas concentrations in baseflow-dominated agricultural streams: implications for surface–ground water interactions and biogeochemistry

**Samuel F. Werner · Bryant A. Browne · Charles T. Driscoll**

Received: 27 May 2010 / Accepted: 8 November 2010 / Published online: 30 November 2010


**Abstract** Small streams that drain agricultural landscapes have come under close scrutiny as potentially significant indirect sources of greenhouse gases (GHGs) to the atmosphere. By exploring the stream-ground water connection in three dimensional space (horizontally and vertically beneath the stream channel, and longitudinally along the stream corridor) our results show (1) ground water can be a significant source of greenhouse gases to streams draining agricultural watersheds with concentrations in excess of atmospheric equilibrium by 221 μmol C $L^{-1}$ carbon dioxide, 0.64 μmol C $L^{-1}$ methane, and 0.65 μmol N $L^{-1}$ nitrous oxide ($N_2O$); (2) changes in the stream-ground water connection can create seemingly erratic patterns in GHG concentrations over short longitudinal distances (order of meters); (3) soil-stream interfaces are hotspots for denitrification and methanogenesis; however, no significant $N_2O$ production was observed at such an interface under a riparian forest; and (4) nitrate ($NO_3^-$) and $N_2O$ can be preserved as electron acceptors in oxic ground waters draining agriculture landscapes; hence, soil nitrification was the major source of $N_2O$ to stream water, with a legacy in ground water dating back to the 1960s; $N_2O$ tracked the seepage of $NO_3^-$ into surface waters. In this study, we demonstrate the utility of detailed measurements of multiple trace gases towards revealing spatial and temporal patterns of surface–ground water interactions and biogeochemistry across several small baseflow-dominated stream ecosystems in central Wisconsin, USA.

**Keywords** Greenhouse gases · Trace gases · Major ions · Surface–ground water interactions · Agriculture · Nitrogen acidification

## Introduction

Evasion of carbon dioxide ($CO_2$), nitrous oxide ($N_2O$), and methane ($CH_4$) from small streams is an important yet poorly documented component of regional and global greenhouse gas budgets (Bowden and Bormann 1986; Kling et al. 1991; Cole et al. 2007). Agriculture plays a major role in the global fluxes of $CO_2$, $N_2O$, and $CH_4$ to the atmosphere (Robertson et al. 2000). Small streams (width 10 m or less) that drain agricultural landscapes have thus come under close scrutiny as potentially significant

Bryant A. Browne—deceased.

S. F. Werner · B. A. Browne
College of Natural Resources, University of Wisconsin Stevens Point, Stevens Point, WI 54481, USA

S. F. Werner (✉) · C. T. Driscoll
Department of Civil and Environmental Engineering, Syracuse University, 151 Link Hall, Syracuse, NY 13244, USA
e-mail: sfwerner@syr.edu

indirect sources of these gases to atmosphere (Nevison 2000; Harrison 2003; Wilcock and Sorrell 2007).

Oversaturation of greenhouse gases (GHGs) in small streams is almost entirely achieved through terrestrial contributions from the watershed. Hydrologic flowpaths (e.g., ground water) supply streams with GHG produced in the surrounding soils and sediments along with allochthonous carbon and nitrogen which can be respired in-stream (Schlesinger et al. 2006; Dawson and Smith 2007). Therefore, knowledge of the hydrologic connection to the adjoining landscape is fundamental to understanding the role of small streams as sources of GHGs. However, quantifying stream-ground water interactions and identifying shifts in biogeochemical processes responsible for GHG production over large spatial scales are considerable challenges (Modica and Reilly 1997; Woessner 2000; Fisher et al. 2004; Lohse et al. 2009; Neill et al. 2006).

In baseflow-dominated streams draining agricultural lands, where the major source of water is from continuous ground water seepage rather than shallow episodic runoff, the potential delivery of GHGs is especially high. Baseflow-dominated streams are prevalent throughout many agriculture drainage basins in the Midwest, USA (Winter et al. 1998). Ground water largely derived from agricultural landscapes has been demonstrated to be a significant source of dissolved nutrients to streams (Kemp and Dodds 2001; Browne and Guldan 2005; Jarvie et al. 2008). Numerous research initiatives have examined the role of stream sediments in the production of GHGs as a result of increased nutrient loading (Hlaváčová et al. 2006; Sanders et al. 2007; Beaulieu et al. 2008); however, the actual contributions of GHGs previously dissolved in ground water have been largely ignored. The role of ground water in supplying GHG gases into agriculture streams, and how such inputs vary in both space and time, remains poorly understood.

The hydrologic connection between ground water and surface water can vary considerably along the stream corridor. Changes in the chemical connection often follow suit, establishing ground water as the decisive factor controlling surface water chemistry in these streams; dissolved gases included. As a consequence, streams receiving ground water seepage sourced from a variety of diverse landscapes (e.g., agriculture, wetland, forest, riparian zones) with different degrees of biogeochemical activity have the capacity to exhibit erratic surface water patterns of trace gas concentrations over longitudinal distances as different flowpaths enter or desist along the stream corridor. Unbeknownst erratic trace gas patterns could instill large errors when scaling up point measurements taken at widely spaced intervals (order of km) to estimate catchment-wide GHG evasion (Reay et al. 2003; Clough et al. 2006).

The challenges of accounting for erratic trace gas patterns may be a research opportunity in some stream ecosystems. As dissolved gases enter streams via groundwater discharge they may be either undersaturated or oversaturated with respect to atmospheric equilibrium due to physical or biological mechanisms. Because such gases behave non-conservatively (e.g., via losses or gains to the atmosphere) within the stream channel (Dawson et al. 1995), their longitudinal patterns can help identify groundwater discharge/recharge patterns along stream corridors (Cook et al. 2003). Furthermore, since gases are involved in many biogeochemical processes (e.g., nitrification, denitrification, methanogenesis), knowing the gaseous composition along a stream corridor may help infer biogeochemical processes controlling water chemistry (Hedin et al. 1998).

The purpose of this study was threefold: (i) investigate the composition of trace gases and dissolved solids of ground waters underlying an agricultural stream; (ii) explore the longitudinal variability in trace gas and dissolved solid concentrations across a variety of different agricultural streams; and (iii) examine the utility of trace gas concentrations for identifying physiochemical stream-ground water connections. A suite of dissolved gases (Ar, $N_2$, $O_2$, $CO_2$, $CH_4$, $N_2O$, CFC11, CFC12, CFC13) coupled with ancillary dissolved solids were employed to this end in several baseflow-dominated agricultural drainage waters across the Midwest (Wisconsin), USA.

## Materials and methods

### Study area

The Little Plover River (LPR) is a baseflow-dominated stream in a predominantly agricultural

sand plain watershed located in central Wisconsin (44° 30′ N, 89° 34′ W), USA (Fig. 1). The third-order stream meanders 10 km in a westerly direction before draining into the Wisconsin River. The 3,000 ha ground water basin of the LPR is recharged by a mixture of different landscapes: agriculture (corn and potato) comprises 44% of the ground watershed with the remainder forest (32%), urban (15%), and grassland (9%). A forested riparian zone buffers the LPR except along a few headwater agricultural drainage ditches and some urban development in the lowest reaches. Stream water quality of the LPR is largely determined by continuous ground water seepage rather than shallow episodic runoff. Of the total runoff (25 cm), 90.0% (22.5 cm) is released as baseflow and 10% (2.5 cm) as direct runoff (Weeks et al. 1965). Longitudinal surveys of trace gases were

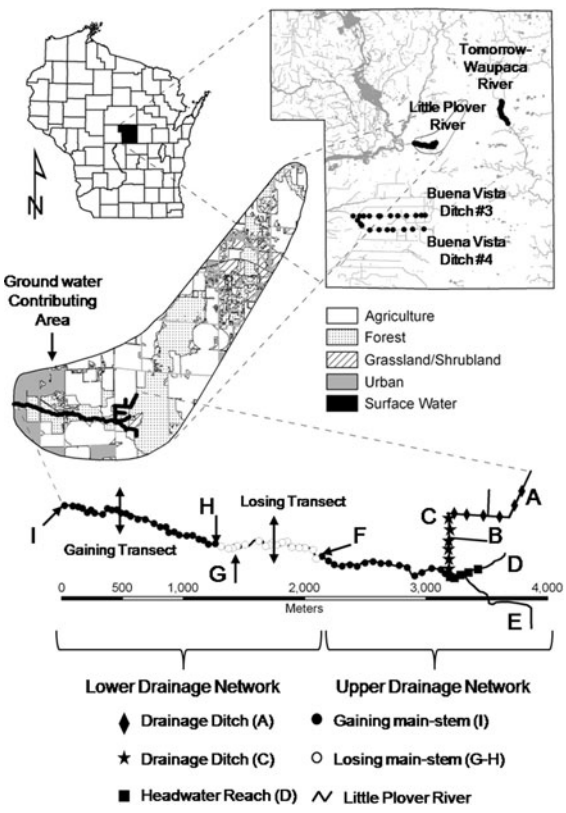


**Fig. 1** Study area and stream surface water sampling network. *Symbols* represent surface water sampling stations; open symbols losing reaches (*white circle*), closed symbols gaining reaches (*diamond*, *star*, *square*, *black circle*). *Arrows*: downstream ends of reaches F–I (as assigned by Browne and Guldan 2005). *Double arrows*: losing and gaining reach subsurface water transects

also conducted in three additional streams: Buena Vista Ditches 3 & 4 (BV 3, BV 4) and a 4.5 km stretch of the Tomorrow-Waupaca River (TWR) (Fig. 1).

Detailed descriptions of the site and hydrologic conditions of the LPR (Browne and Guldan 2005), BV 3 & 4 (River Alliance of Wisconsin 2009), and the TWR (Guldan 2004) can be found elsewhere. Briefly, the LPR drainage network consists of headwater agricultural ditches (Reaches A–E) that drain into the third-order main branch (Reaches F–I) as assigned by Browne and Guldan (2005). The upper drainage network includes five agricultural drainages (Reaches A–E) and a section of natural meander (Reach F). The lower drainage network includes three reaches (G, H, I) partitioned to identify important breakpoints in the hydraulic connection with landscape. Reaches G and H are permanent and intermittent losing reaches, respectively, where ground water is recharged by surface water (i.e., by ground water previously discharged in upstream reaches, which potentially equilibrates with modern atmosphere within the stream channel). Reach I is an intense gaining reach where a major portion of the LPR's baseflow is derived.

## Experimental design

A network of minipiezometers at the ground water-surface water interface was used to determine the concentrations of dissolved organic carbon (DOC), $NO_3^-$, and dissolved gases (Ar, $N_2$, $O_2$, $CO_2$, $CH_4$, $N_2O$, CFCs) of ground waters underlying the LPR. Lateral and vertical transects (Fig. 1) were established (i) across a gaining stream reach to capture the tail end of ground water flowpaths as they discharged to the LPR; and (ii) across a losing stream reach to assess the biogeochemical processes of the underlying stream sediments. Minipiezometers were constructed from polyethylene tubing (0.43 cm i.d., 0.63 cm o.d.). Wells screens, composed of 8–10 lines of perforations 2.5 cm long, were fabricated by four or five passes through a sewing machine. A retractable tempered stainless steel insertion rod was used to position the well screens at depth intervals of 0.50 m, 1 m, and 1.5 m below the stream-sediment interface or land surface. Minipiezometers ($n = 59$) installed in the gaining transect spanned 42 m laterally bank to bank across the near-stream zone (Fig. 2). Minipiezometers

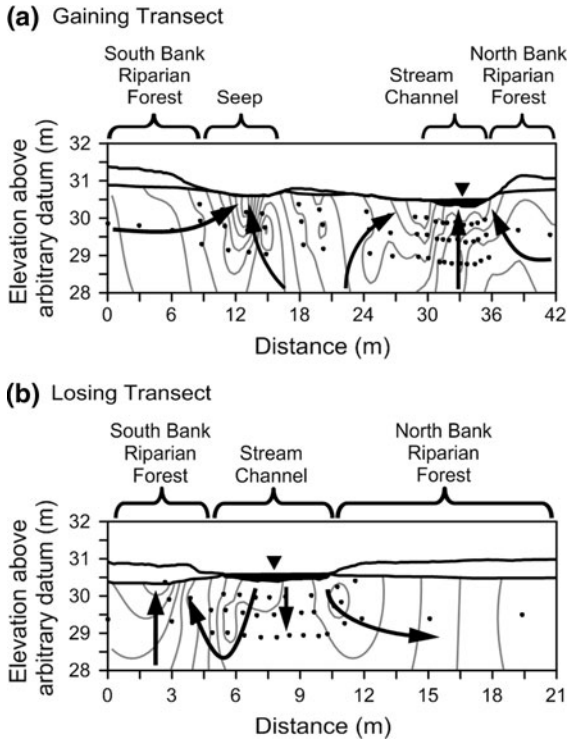


**Fig. 2** Little Plover River subsurface water transects **a** gaining reach, **b** losing reach. *Solid gray lines* indicate equipotentials (5 cm interval for gaining, 3 cm interval for losing) and *arrows* indicate dominant flowpaths. Location of minipiezometers denoted by closed circles

($n = 37$) installed in the losing section spanned 21 m (Fig. 2). Standard surveying procedures were used to measure land surface topography across transects with the stream water level serving as the bench mark. Hydrologic gradient measurements of ground waters sampled from minipiezometers are described in Browne and Guldan (2005).

Longitudinal samples of LPR stream surface water ($n = 79$) were sited at 60 m intervals along the stream thalweg extending into several headwater tributaries (Fig. 1). Sites were in close proximity to the minipiezometers network used in the synoptic survey of Browne and Guldan (2005). Unfortunately, the Browne and Guldan (2005) minipiezometers infrastructure deteriorated (bio-fouling, missing/damaged) beyond practical use at the time of this study. Reconstruction of this minipiezometer network was deemed too costly an undertaking. Therefore, ground water seepage, cumulative seepage, and actual stream flow measurements (sampled 27 June 2000) of Browne and Guldan (2005) reported in this study are for comparison purposes only. Ostensibly, the "27 June 2000" data set provides a 'historic' record of the LPR stream-ground water hydrologic connection; possible differences in the hydrologic conditions at the time of this study are acknowledged.

Surface water samples of the LPR were collected at baseflow conditions 5–13 June 2006 during day light hours (10:00–17:00). No storm event (precipitation >0.5 cm) occurred during the sampling campaign. Additional longitudinal surveys of stream surface water trace gas concentrations were conducted in (i) BV 3 ($n = 11$) at 1 km intervals 6 Jan 2006; (ii) BV 4 ($n = 11$) at 1 km intervals 9 Jan 2000; and (iii) 4.5 km stretch of the TWR ($n = 24$) at 200 m intervals 10–16 Jan 2006 (Table 1). Little Plover River gaining and losing transects were sampled 9–10 April 2006.

## Analytical methods

Ground water samples were collected using a peristaltic pump attached directly to the minipiezometers. Field measurements were obtained with an YSI 650 MDS sonde (temperature, pH, specific conductance, and dissolved oxygen) (Yellow Springs, OH, USA) and a Common Sensing (Clark Fork, ID, USA) total dissolved gas probe. Both were equipped with flow through cells to avoid atmospheric exposure during measurement. Sample collection, filtration, and preservation for dissolved solids were performed according to Wisconsin Department of Natural Resource protocols (WDNR 1996). Standard laboratory procedures (APHA 1995) were used for Ca, Mg, K, Na, Si, $F^-$, $SO_4^{2-}$, $Cl^-$, $NO_3^-$, $NH_4^+$, soluble reactive phosphorus (SRP), acid neutralizing capacity (ANC), dissolved organic carbon (DOC), and dissolved inorganic carbon (DIC analyses) (Table 2).

Dissolved gases (Ar, $N_2$, $O_2$, $CO_2$, $CH_4$, $N_2O$, CFC11, CFC12, CFC13) were collected as gas samples ($n = 3$) in the field using pumping induced ebullition (PIE) (Browne 2004; Browne and Guldan 2005). (*Ebullition* is the spontaneous formation of bubbles when the total dissolved gas pressure exceeds the hydrostatic pressure). Each 30 mL replicate sample was compressed into a 12 mL serum bottle fitted with thick (20 mm) butyl stopper and analyzed within 48 h. Sample integrity over prolonged storage

**Table 1** Descriptive statistics (coefficient of variation expressed as a percentage, %CV) for longitudinal surveys of stream surface water dissolved oxygen (DO, percent saturation), excess carbon dioxide ($xsCO_2$), excess nitrous oxide ($xsN_2O$), and excess methane ($xsCH_4$) concentrations in baseflow-dominated agricultural streams, central Wisconsin, USA

| Stream | Channel[a] Width (m) | Collection Date | Station Interval | *n* | Dissolved gas[b] | Mean (%CV) | Minimum | Maximum |
|---|---|---|---|---|---|---|---|---|
| LPR | 2.0 | 10–16 June 2006 | 60 m | 79 | DO (% Sat) | 90.1 (13) | 63.5 | 111.2 |
| | | | | | $xsCO_2$ (μmol C $L^{-1}$) | 52.1 (76) | 12.6 | 183.0 |
| | | | | | $xsN_2O$ (μmol N $L^{-1}$) | 0.12 (103) | 0.01 | 0.31 |
| | | | | | $xsCH_4$ (μmol C $L^{-1}$) | 0.15 (80) | 0.02 | 0.64 |
| TWR | 4.5 | 16–17 January 2006 | 200 m | 24 | DO (% Sat) | 91.5 (3) | 87.4 | 96.4 |
| | | | | | $xsCO_2$ (μmol C $L^{-1}$) | 42.1 (19) | 21.3 | 52.9 |
| | | | | | $xsN_2O$ (μmol N $L^{-1}$) | 0.03 (30) | 0.01 | 0.04 |
| | | | | | $xsCH_4$ (μmol C $L^{-1}$) | 0.11 (32) | 0.02 | 0.15 |
| BV 3 | 3.5 | 6 January 2006 | 1 km | 11 | DO (% Sat) | 75.3 (9) | 61.1 | 80.9 |
| | | | | | $xsCO_2$ (μmol C $L^{-1}$) | 101.7 (42) | 47.2 | 166.8 |
| | | | | | $xsN_2O$ (μmol N $L^{-1}$) | 0.17 (113) | 0.02 | 0.659 |
| | | | | | $xsCH_4$ (μmol C $L^{-1}$) | 0.10 (70) | 0.01 | 0.26 |
| BV 4 | 4.0 | 9 January 2006 | 1 km | 11 | DO (% Sat) | 78.9 (6) | 72.0 | 85.2 |
| | | | | | $xsCO_2$ (μmol C $L^{-1}$) | 115.8 (65) | 18.4 | 221.9 |
| | | | | | $xsN_2O$ (μmol N $L^{-1}$) | 0.05 (57) | <0.01 | 0.11 |
| | | | | | $xsCH_4$ (μmol C $L^{-1}$) | 0.11 (81) | 0.02 | 0.25 |

[a] Average stream channel width of surveyed sections

[b] 'Excess' gas is the concentration of gas above or below atmospheric equilibrium (concentration = 0 at equilibrium, undersaturated <0, supersaturated >0) as determined by Henry's law, adjusting measured dry mole fractions for their respective atmospheric mixing ratios ($CO_2$ 380 ppmv, $CH_4$ 1.75 ppmv, $N_2O$ 315 ppbv)

**Table 2** Analytical methods employed in this study; chlorofluorocarbons (CFCs); soluble reactive phosphorus (SRP); dissolved organic carbon (DOC); dissolved inorganic carbon (DIC); acid neutralizing capacity (ANC)

| Analyses | Methods | Reference |
|---|---|---|
| $N_2$ and Ar | Membrane inlet mass spectroscopy | Hiden Analytical |
| CFCs | Gas chromatography, ECD | Bullister and Weiss (1988) |
| $N_2O$ | Gas chromatography, ECD | Gleason et al. (2009) |
| $CO_2$ and $CH_4$ | Gas chromatography, methanizer-FID | Gleason et al. (2009) |
| Ca and Mg | Atomic absorption spectroscopy | APHA (1995) |
| K and Na | Flame emission spectroscopy | APHA (1995) |
| $F^-$, $Cl^-$, and $SO_4^{2-}$ | Ion chromatography | Dionex application note 133 |
| $NO_3^- + NO_2^-$ | Cd reduction-sulfanilamide | Lachat method #10-107-04-1-A |
| $NH_4^+$ | Phenol-hypochlorite | Lachat method #10-107-06-1-C |
| SRP | Molybdate-ascorbic acid | Lachat method #10-115-01-1-A |
| Si | Colorimetric, molybdate blue | USGS I-1700-85 |
| DOC | Wet oxidation with NDIR detection | Shimadzu |
| DIC | Phosphoric acid with NDIR detection | Shimadzu |
| ANC | Titration, bromocresol green-methyl red | APHA (1995) |

for most gases remained unchanged >10 days. One replicate ($n = 1$) was dedicated to each of the three gas analytical methods (Table 2).

Dry gas mole fractions (X) corrected for PIE fractionation (Browne, 2004) were determined by gas chromatography and mass spectrometry. Argon, $O_2$,

and $N_2$ were measured using a Hiden HPR-20 QIC membrane inlet mass spectrometer (MIMS) (Warrington, UK). Nitrous oxide was detected with an electron capture detector (ECD), and $CH_4$ and $CO_2$ (after methanization) with a flame ionization detector (FID) using a SRI Model 8610 GC (Torrance CA, USA). Chromatographic conditions for $N_2O$, $CH_4$, and $CO_2$ described by Gleason et al. (2009) and references therein, provide minimum detection limits of <3 ppbv $N_2O$ (ECD), <10 ppbv $CH_4$ (FID), and <1 ppmv $CO_2$ (FID). Chlorofluorocarbons (CFC11, CFC12, CFC113) were measured with an ECD on a Hewlett Packard 5890 GC (Santa Clara, CA, USA) under chromatographic conditions described by Bullister and Weiss (1988). Gas chromatographs were calibrated and verified with commercial $N_2O$, $CH_4$, and $CO_2$ air blends and a reference standard from the National Oceanic and Atmospheric Administration.

The dissolved concentration of each gas at the field water temperature was obtained by Henry's Law calculation:

$$C = K_{\mathrm{H,field}} \times \mathrm{X} \times (P_{\mathrm{T}} - w) \quad (1)$$

where $C$ is the dissolved concentration of the gas in mol $L^{-1}$, $K_{\mathrm{H,field}}$ is the gas specific Henry's Law constant at field temperature and $P_{\mathrm{T}}$ and $w$ are the total dissolved gas pressure (MPa) and the field temperature water vapor pressure (MPa), respectively. The $K_{\mathrm{H}}$ values were obtained from temperature-dependent solubility data in Wilhelm et al. (1977) for Ar, $N_2$, $O_2$, $CO_2$, $N_2O$; and $CH_4$, from Warner and Weiss (1985) for CFC11 and CFC12; and from Bu and Warner (1995) for CFC113. Dissolved concentrations of $CO_2$, $CH_4$, and $N_2O$ are reported in terms of 'excess' gas (i.e., *xs*$CO_2$): the concentration of gas above or below atmospheric equilibrium (concentration = 0 when at equilibrium, undersaturated <0, and oversaturated >0). Excess gas concentrations were determined by Eq. 1 after correcting the measured dry mole fractions for their respective atmospheric mixing ratios ($CO_2$ 380 ppmv, $CH_4$ 1.75 ppmv, $N_2O$ 315 ppbv).

The total concentration of dissolved $N_2$ in ground waters was partitioned between atmospheric and biogenic sources (Böhlke and Denver 1995; Vogel et al. 1981; Martin et al. 1995) using a four-step Henry's Law approach described in detail by Browne et al. (2008). Briefly, excess air (oversaturation by dissolution of entrapped air bubbles during recharge, Heaton and Vogel 1981; Holocher et al. 2003) was negligible in all samples (Browne and Guldan 2005). Argon based apparent recharge temperature was used to select a Henry's Law constant to calculate $N_2$ concentration of air-saturated water (ASW). Biogenic $N_2$ was determined by the difference between total $N_2$ and $N_2$ of ASW. Biogenic $N_2$ can be reliably measured above a nominal concentration of 17 μmol $L^{-1}$ by a combination of PIE sampling and MIMS.

Apparent CFC recharge age-dates for ground waters were obtained using a Henry's Law approach (Plummer and Busenberg 2000). Dry gas mole fractions (in parts per trillion by volume, pptv) of CFC11, CFC12, and CFC113 at the time of recharge were obtained using the following relationship:

$$\mathrm{X}_{\mathrm{rech}} = \left(\frac{K_{\mathrm{H,field}}}{K_{\mathrm{H,rech}}}\right)\left(\frac{P_{\mathrm{T}} - w}{P}\right)\mathrm{X} \quad (2)$$

where $P$ is the general atmospheric pressure (MPa) based on elevation; and the $K_{\mathrm{H}}$ values represent Henry's Law constants at the field temperature and the apparent recharge temperature. Dry air mole fractions of CFC11, CFC12, CFC113 obtained by Eq. 2 were referenced to chronological records of atmospheric mixing ratios for CFCs to determine a unique "apparent" ground water age-date or recharge date. A more through discussion on the apparent CFC recharge age-dates methodology can be found in Browne and Guldan (2005) and references therein.

Atmospheric CFC contamination in stream surface water precludes the use of apparent CFC recharge age-dates estimates of the surface water column. Alternatively, a CFC index was developed to determine the relative degree of atmospheric equilibrium amongst CFC12, CFC11, and CFC113 in the stream surface water using the following relationship:

$$\bar{\mathrm{I}}_{\mathrm{CFC}} = -\log\left(\frac{\mathrm{X}_{\mathrm{stream}}}{\mathrm{X}_{\mathrm{modern}}}\right) \quad (3)$$

where X represents the dry air mole CFC fractions measured in the stream and modern air. The CFC indices of CFC12, CFC11, and CFC113 were then averaged to yield a mean CFC index ($\bar{\mathrm{I}}_{\mathrm{CFC}}$). Hence, stream water with a $\bar{\mathrm{I}}_{\mathrm{CFC}}$ value = 0 is in equilibrium with the modern atmosphere, CFC undersaturated when $\bar{\mathrm{I}}_{\mathrm{CFC}} > 0$ (e.g., 'old water'), and CFC oversaturated when $\bar{\mathrm{I}}_{\mathrm{CFC}} < 0$.

Statistics and graphics

All statistical analyses were performed with SAS (version 9.2, SAS Institute, Cary, NC, USA). Color image maps were created in Surfer (version 9, Golden Software Inc., Golden, CO, USA) using a Kriging gridding method with interpolated pixels. [*Note*: the color image maps presented in this paper have interpolated pixels. Stream water chemistry is thus interpolated down into the underlying sediments despite the upward movement of ground water into the stream in the gaining transect. The chemical contributions of the underlying stream sediments were not measured and are unknown but not to be discounted; caution must be exercised when interpreting the chemistry in this regard].

## Results

Hydrologic flow paths

The hydrologic conditions of the LPR are reported in Browne and Guldan (2005). Agreement between cumulative discharge across stream segments with actual stream flow showed that the stream-ground water connection was well characterized by the ground water seepage measurements (Fig. 3). Ground water seepage in the upper drainage network (0–2.2 km) and the gaining reach of the lower drainage network (3.0–4.5 km) provided a nearly continuous contribution to stream flow. A relatively intense zone of ground water seepage was centered at 3.5 km downstream. This known pattern of ground water discharge/recharge provided a platform to understand the chemical patterns in LPR surface water.

Cross sectional distributions of hydrologic heads outline the predicted flowpaths of ground water into the gaining reach (Fig. 2a) and out of the losing reach (Fig. 2b). Gaining and losing transects were buffered by forested riparian zones along both sides of the stream corridor. Across the middle of the gaining reach transect, a water table was observed at the land surface establishing several seepage zones. Most notable was an area of intense ground water upwelling into a land depression (relict stream channel). Predicted flow paths revealed vertical up-welling of deeper ground water directly beneath the gaining reach stream channel and under the south bank of the losing reach. Vertical down-welling of stream surface water was observed directly under the losing stream channel. Horizontal flow of subsurface water parallel to the land surface was found under the south bank of the gaining reach.

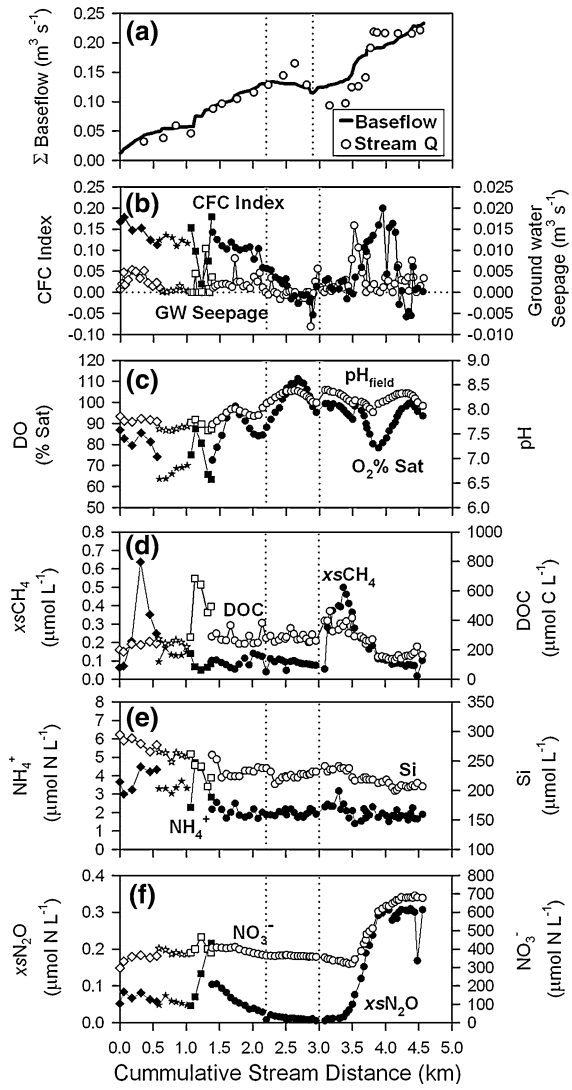


**Fig. 3** Little Plover River surface water chemistry **a** baseflow calculated from cumulative ground water seepage (*solid line*) and measured stream flow for 27 June 2000, **b** CFC index and ground water seepage, **c** dissolved oxygen percent saturation and pH, **d** excess methane and dissolved organic carbon, **e** ammonium and silica, **f** excess nitrous oxide and nitrate. Samples for water chemistry collected 5–13 June 2006. The *hashed vertical lines* (2.2 and 3.0 km) reference the extent of the losing reach. *Black symbols* correspond to left vertical axis, *open symbols* correspond to right vertical axis

Apparent CFC recharge age-dates for ground waters underlying the gaining reach spanned nearly four decades (1965–2000) with a mean age of 27 years (ca. 1978) (Fig. 4h). The oldest ground water up-welled directly under the stream channel; the youngest ground water (ca. 2000) occurred near the seep at the riparian forest indicating an input of subsurface water sourced from a local shallow flow path. The majority of the ground water flowpaths exhibited recharge dates close to the mean (ca. 1978) (Table 3). The CFC age-dates for ground waters sampled in the gaining reach all translate into $\bar{I}_{CFC}$ values $> 0$ (i.e., CFC undersaturation with respect to modern air).

Recharge age-dates for ground waters underlying the losing reach spanned 25 years (1976–2001) with a mean age of 21 years (ca. 1985) (Fig. 5h). The oldest ground waters were observed just below the water table at either side of the stream channel. The youngest ground water (ca. 2001) was found directly under the stream channel. The majority of the ground waters underlying this losing reach of the LPR exhibited recharge dates from the late 1980s. The apparent lack of modern water within the subsurface waters suggests a mixing of older regional up-welling ground water with modern down-welling stream water.

## Spatial patterns in subsurface water chemistry

Chemical variations in ground water were highly organized across the gaining transect, with the most marked changes in concentrations occurring in a direction perpendicular to the stream from the south bank (Fig. 4). Concentrations of electron acceptors ($O_2$, residual $NO_3^-$, and $N_2O$) were elevated in the

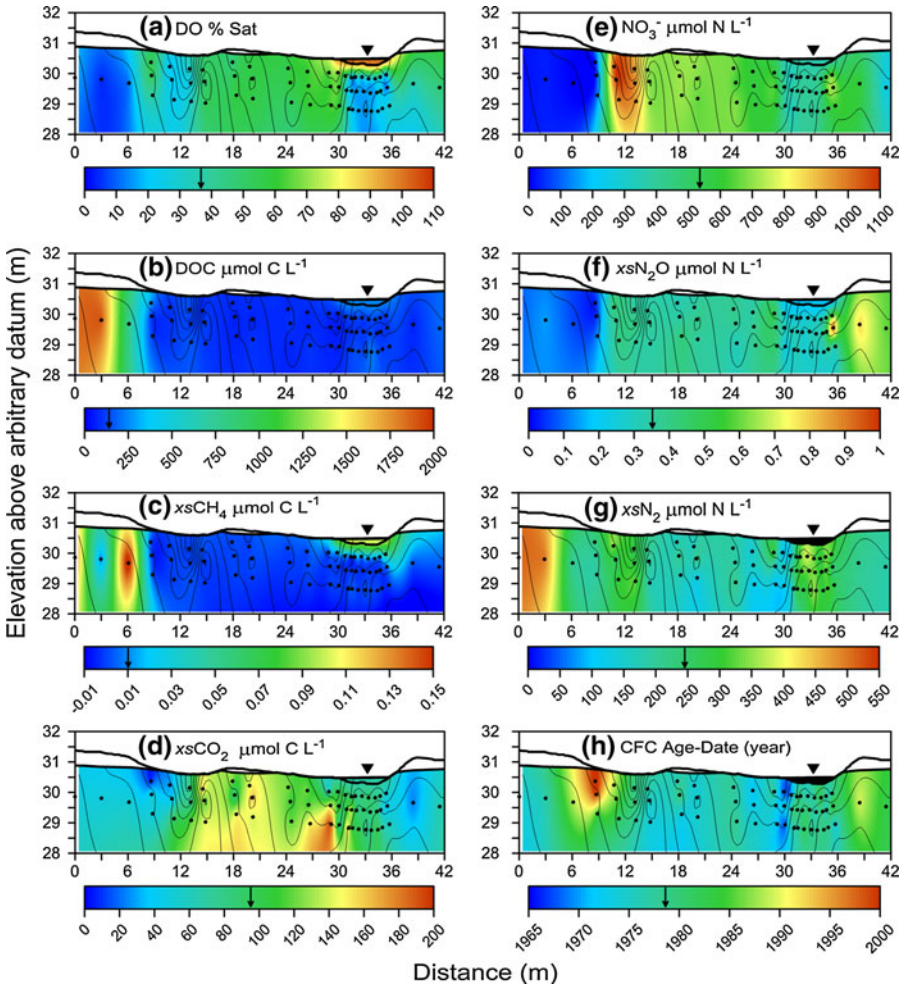


**Fig. 4** Little Plover River gaining reach subsurface water chemistry for 9–10 April 2006 including **a** dissolved oxygen percent saturation, **b** dissolved organic carbon, **c** excess methane, **d** excess carbon dioxide, **e** residual nitrate, **f** excess nitrous oxide, **g** excess "biogenic" dinitrogen, and **h** apparent CFC age-date. Arrow within color scale indicates parameter mean. Solid gray lines indicate equipotentials (5 cm interval). Location of minipiezometers denoted by closed circles. *Black fill* indicates stream surface water chemistry was not included in the Kriging procedure. Color figures available online

**Table 3** Descriptive statistics (standard deviation, *s*) for CFC age-date (year), dissolved oxygen (DO, percent saturation), dissolved organic carbon (DOC), excess methane ($xsCH_4$), excess carbon dioxide ($xsCO_2$), nitrate ($NO_3^-$), excess nitrous oxide ($xsN_2O$), and excess "biogenic" dinitrogen ($xsN_2$) concentrations of ground waters and stream surface water across gaining and losing reach vertical and lateral transects of the Little Plover River, Wisconsin, USA (April 9–10, 2006)

| Site | CFC Date (year) | DO (% Sat) | DOC (μmol C $L^{-1}$) | $xsCH_4$[a] (μmol C $L^{-1}$) | $xsCO_2$[a] (μmol C $L^{-1}$) | $NO_3^-$ (μmol N $L^{-1}$) | $xsN_2O$[a] (μmol N $L^{-1}$) | $xsN_2$[b] (μmol N $L^{-1}$) |
|---|---|---|---|---|---|---|---|---|
| Gaining reach | | | | | | | | |
| Mean | 1978 | 36.0 | 172 | 0.01 | 94.7 | 528.3 | 0.34 | 246.2 |
| (*s*) | (7) | (18.9) | (338) | (0.03) | (41.3) | (256.8) | (0.16) | (93.8) |
| Minimum | 1965 | 4.0 | 37 | −0.01 | 2.0 | 1.2 | 0.02 | 87.0 |
| Maximum | 2001 | 67.8 | 1912 | 0.17 | 200.8 | 1089.3 | 1.09 | 514.0 |
| Stream | – | 100.3 | 239 | 0.10 | 68.4 | 365.8 | 0.17 | – |
| Losing reach | | | | | | | | |
| Mean | 1985 | 12.5 | 335 | 0.45 | 229.4 | 254.8 | 0.24 | 274.4 |
| (*s*) | (7) | (11.3) | (120) | (1.13) | (88.4) | (127.9) | (0.17) | (98.4) |
| Minimum | 1976 | 2.2 | 212 | −0.01 | 128.2 | 1.1 | −0.01 | 40.6 |
| Maximum | 2001 | 41.1 | 831 | 4.10 | 510.6 | 391.4 | 0.65 | 535.5 |
| Stream | – | 108 | 70 | 0.06 | 0.14 | 391.6 | < 0.01 | – |

[a] 'Excess' gas is the concentration of gas above or below atmospheric equilibrium (concentration = 0 at equilibrium, undersaturated < 0, supersaturated > 0) as determined by Henry's law, adjusting measured dry mole fractions for their respective atmospheric mixing ratios ($CO_2$ 380 ppmv, $CH_4$ 1.75 ppmv, $N_2O$ 315 ppbv)

[b] $xsN_2$ is 'excess' $N_2$ of biogenic origin (i.e., denitrification) determined by the difference between total measured $N_2$ and $N_2$ of air saturated water (calculated from argon based apparent recharge temperature)

near-stream environment while concentrations of electron donors (DOC, $CH_4$) and biogenic $N_2$ ($xsN_2$) were elevated more inland (Fig. 4). The spatial organization of electron donors and electron acceptors became less apparent in ground waters near the stream channel. Here, dissolved oxygen (DO, percent saturation) was depleted (DO < 25% Sat) yet there were low concentrations of DOC and $xsCH_4$ (<200 and 0.01 μmol C $L^{-1}$, respectively) with concurrently elevated concentrations of residual $NO_3^-$, $xsN_2O$, and $xsN_2$ (>400, 0.3, and 250 μmol N $L^{-1}$, respectively). All gaining reach ground waters contained at least some quantity of $xsN_2$ (>87.0 μmol N $L^{-1}$) (Table 3). Shallow anoxic young ground water beneath the riparian forest contained considerably less dissolved solids than deeper oxic old ground water up-welling beneath the stream channel.

Chemical variations in losing reach ground waters were also highly organized, predominantly around the stream channel (Fig. 5). Dissolved oxygen was depleted (<10% Sat) just below the water table at either side of the stream channel and at depth several meters beneath the stream bed. Coincident were elevated $xsCH_4$ (2.75 μmol C $L^{-1}$) and low residual $NO_3^-$ (<10 μmol N $L^{-1}$) concentrations. However, DOC was relatively uniform (300–400 μmol C $L^{-1}$) across the entire transect. Nitrous oxide concentrations were near atmospheric equilibrium below the stream bed and become increasingly oversaturated with depth. Initial $NO_3^-$ concentrations (the sum of residual $NO_3^-$ and excess $N_2$) of ground waters just below the stream bed were close to that of stream surface water (365 μmol N $L^{-1}$) but increased to more than 700 μmol N $L^{-1}$ in the deeper minipiezometers suggesting a non-stream (e.g., regional) source of ground water (data not shown).

Correlations between different electron donors and acceptors revealed several strong and predictable relationships (Fig. 6). First, we found a strict inverse relationship between $xsCH_4$ and DO for all ground waters (gaining and losing) (Fig. 6g). Second, we found a weak negative correlation ($r^2 = 0.17$, $P \leq 0.001$) between $xsN_2$ and DO (data not shown) in losing ground waters which strengthen ($r^2 = 0.55$, $P < 0.001$) in gaining ground waters. Third, we found strong and inverse relationships between DOC and (i) DO (Fig. 6a); (ii) oxidized forms of N (i.e., $NO_3^-$ and $N_2O$, Fig. 6c, d). Closer examination of

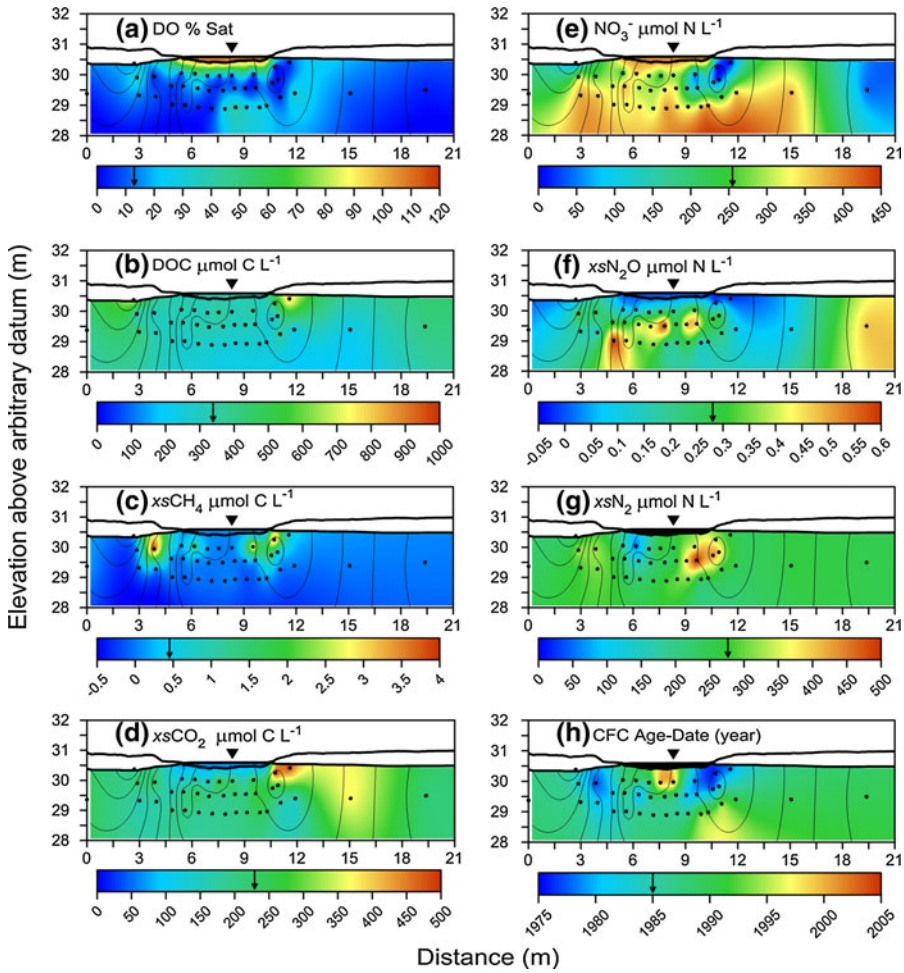


**Fig. 5** Little Plover River losing reach subsurface water chemistry for 9–10 April 2006 including **a** dissolved oxygen percent saturation, **b** dissolved organic carbon, **c** excess methane, **d** excess carbon dioxide, **e** residual nitrate, **f** excess nitrous oxide, **g** excess "biogenic" dinitrogen, and **h** apparent CFC age-date. Arrow within color scale indicates parameter mean. Solid gray lines indicate equipotentials (3 cm interval). Location of minipiezometers denoted by closed circles. Black fill indicates stream surface water chemistry was not included in the Kriging procedure. Color figures available online

these relationships revealed that residual $NO_3^-$ and $N_2O$ only persisted in ground waters that contained low concentrations of DOC (<500 µmol C $L^{-1}$). Hence, ground waters with DOC concentrations >500 µmol C $L^{-1}$ never exhibited any accumulation of residual $NO_3^-$ above 50 µmol N $L^{-1}$ or *xs*$N_2O$ above 0.15 µmol N $L^{-1}$. Instead, *xs*$N_2$ was the predominant form of N in ground waters which contained >500 µmol C $L^{-1}$ of DOC.

Despite the strong and inverse relationships between different N species and DOC, correlations between nitrogen redox couples (e.g., *xs*$N_2O$, residual $NO_3^-$, and *xs*$N_2$) were less apparent. Only between *xs*$N_2O$ and residual $NO_3^-$ (Fig. 6h) was there any significant correlation ($r^2 = 0.31$, $P < 0.0001$) in gaining reach ground waters. However several notable relationships arose when denitrification progression was considered (Fig. 7). Denitrification progression is the ratio of excess N to initial N expressed as a percentage (e.g., 100% indicates all of the initial $NO_3^-$ was converted to excess $N_2$). Despite $N_2O$ showing no correlation with excess $N_2$, there was a weak but significant negative relationship ($r^2 = 0.33$, $P < 0.0001$) between *xs*$N_2O$ and denitrification progression (Fig. 7b). Moreover, *xs*$CH_4$ only accumulated when denitrification was close to 100% (e.g., all the initial $NO_3^-$ was consumed). This pattern suggests $N_2O$ was only consumed under intense denitrifying conditions and $NO_3^-$ had the capacity to poise the redox status.

Correlations between apparent CFC recharge age-dates and N species were also poor. Nonetheless, several notable observations can be made. First, the legacy of $N_2O$ (*xs*$N_2O$ > 0.25 µmol N $L^{-1}$) laden ground water dates as far back as 1965 (Fig. 8b). Second, there is a bimodal relationship between

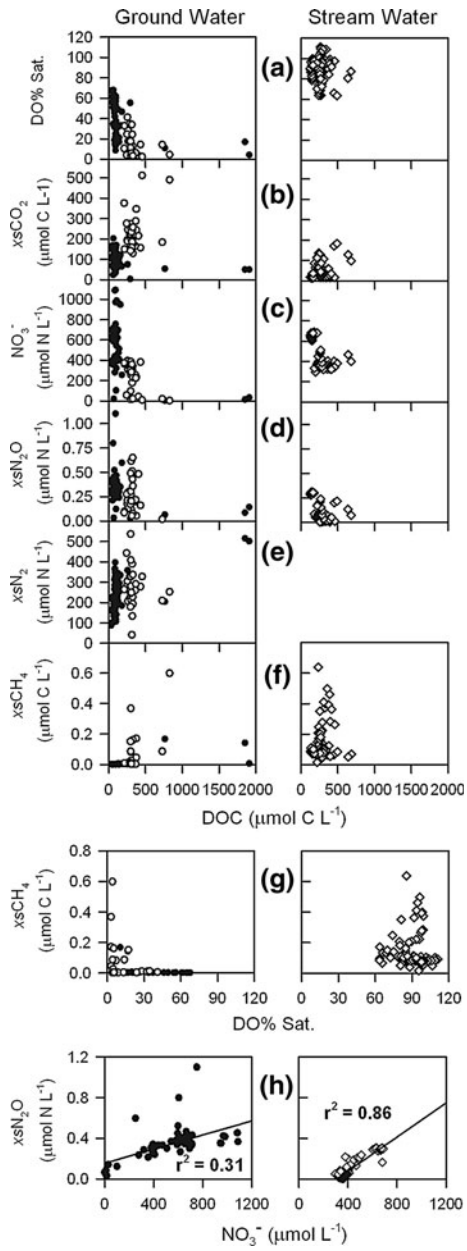


**Fig. 6** Ground-stream water correlations between **a–f** dissolved organic carbon and dissolved oxygen percent saturation, excess carbon dioxide, residual nitrate, excess nitrous oxide, excess "biogenic" dinitrogen, and excess methane; respectively, **g** dissolved oxygen percent saturation and excess methane, and **h** residual nitrate and excess nitrous oxide. Gaining reach ground water (*closed circle*), losing reach ground water (*open circle*), and stream surface water (*open diamond*). All reported correlations significant at $P < 0.0001$

initial $NO_3^-$ and ground water age. Very old (<1970) and young (>1990) ground water received less N inputs than moderately aged (1970–1990) ground

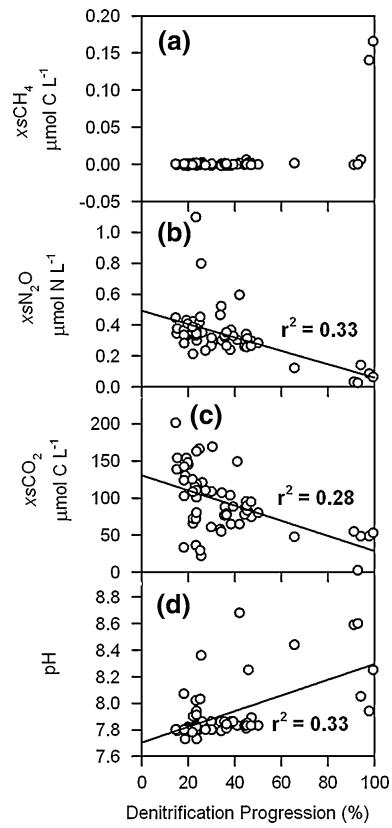


**Fig. 7** Correlations between denitrification progression and **a** excess methane, **b** excess nitrous oxide, **c** excess carbon dioxide, and **d** pH. Denitrification progression is the ratio of excess N to initial N (excess N plus residual N) expressed as a percentage (e.g., 100% indicates all of the initial $NO_3^-$ was converted to excess $N_2$). All reported correlations significant at $P < 0.0001$

water (Fig. 8d). Third, both excess $N_2$ (not shown) and denitrification progression did not increase with ground water residence time; rather, denitrification progression was furthest along in more recent ground water and positively correlated ($r^2 = 0.28$, $P < 0.0001$) with recharge date (Fig. 8e).

The spatial organization of DIC concentrations in gaining reach ground waters was weakly correlated to the presence of residual $NO_3^-$ ($r^2 = 0.26$, $P < 0.0001$) In gaining reach ground waters, the highest concentrations of $xsCO_2$ were found in between the seep and the stream channel (coinciding with high $NO_3^-$ concentrations) (Fig. 4d). Excess $CO_2$ concentrations here were >120 µmol C $L^{-1}$ compared to 40 µmol C $L^{-1}$ of the ground waters beneath the opposing banks. This three-fold difference in $CO_2$

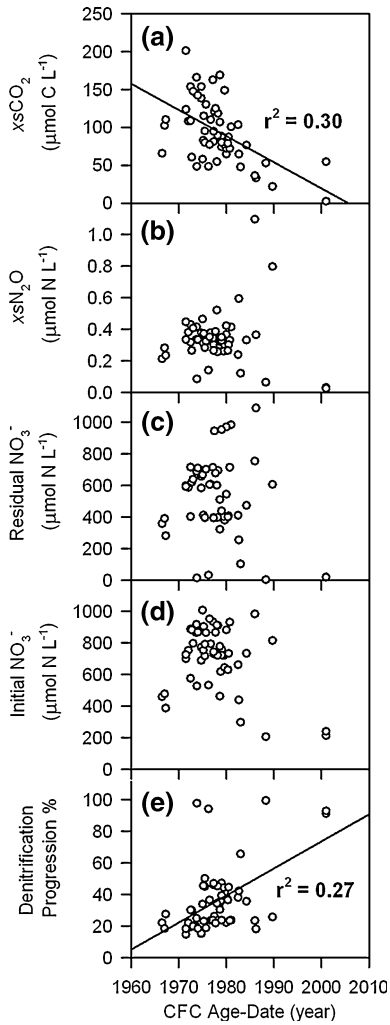


**Fig. 8** Correlations between apparent CFC age-date and **a** excess carbon dioxide, **b** excess nitrous oxide, **c** residual nitrate, **d** initial nitrate, and **e** denitrification progression. Denitrification progression is the ratio of excess N to initial N (excess N plus residual N) expressed as a percentage (e.g., 100% indicates all of the initial $NO_3^-$ was converted to excess $N_2$). All reported correlations significant at $P < 0.0001$

was attributed to relatively lower pH values, higher DIC concentrations of the ground waters up-welling in the middle portion of the transect (data not shown). Increases in pH ($r^2 = 0.33$, $P < 0.0001$) and subsequent decreases in $CO_2$ concentrations ($r^2 = 0.28$, $P < 0.0001$) were weakly correlated with denitrification progression (Fig. 7c–d). Despite the increase in pH, all ground waters remained undersaturated with respect to the solubility of carbonate minerals (i.e., calcite) (data not shown).

## Spatial patterns in stream water chemistry

The known pattern of ground water discharge/recharge provided a platform to inform the chemical patterns in LPR stream water (Figs. 3, 9). Gaining sections were undersaturated ($\bar{I} > 0$) with CFCs indicative of the entry of old groundwater where as the losing reach was near or at equilibration with the modern atmosphere ($\bar{I} = 0$) (Fig. 3a). However there were notable exceptions; for example, at 3.5 km downstream a relative intense area of ground water seepage was not accompanied by a large increase in the CFC index suggestive of local shallow subsurface flow. Although highly variable, the CFC index was consistent with the groundwater seepage pattern: points of ground water entry were characterized by values of $\bar{I} > 0$.

The high degree of variability in the CFC index herald substantial variation in stream water chemistry over longitudinal distances. Different physical and chemical interactions between ground water and stream water revealed several fundamental relationships between dissolved gases and solids (Figs. 3, 9). First, most dissolved gases (i.e., CFCs, $CH_4$, $N_2O$, $CO_2$) approached atmospheric equilibrium in the losing reach, while dissolved solid concentrations remained relatively unchanged. Second, steep changes in $NO_3^-$ concentrations were accompanied by elevated concentrations of $N_2O$ in gaining reaches (Fig. 3f). Third, fluctuations in DO and $CO_2$ were closely mimicked by changes in hydrogen ion concentrations (Fig. 3c).

The predicable relationships found between different electron donors and acceptors in ground waters were absent in stream water (Fig. 6). Most notable was the lack of the strict inverse relationship between $CH_4$ and DO in stream water. Rather, several new relationships between electron acceptors and donors emerged. For example, there was a strong negative linear correlation between $xsCO_2$ and DO ($r^2 = 0.61$, $P < 0.0001$) (data not shown). However, there was one chemical correlation in ground waters which was reinforced in stream water. The weak positive linear correlation between $N_2O$ and $NO_3^-$ strengthen from $r^2 = 0.31$ in gaining reach ground waters to $r^2 = 0.86$ in stream waters (Fig. 6h).

Changes in the stream-ground water physiochemical connection along the stream corridor established several prominent longitudinal patterns in stream

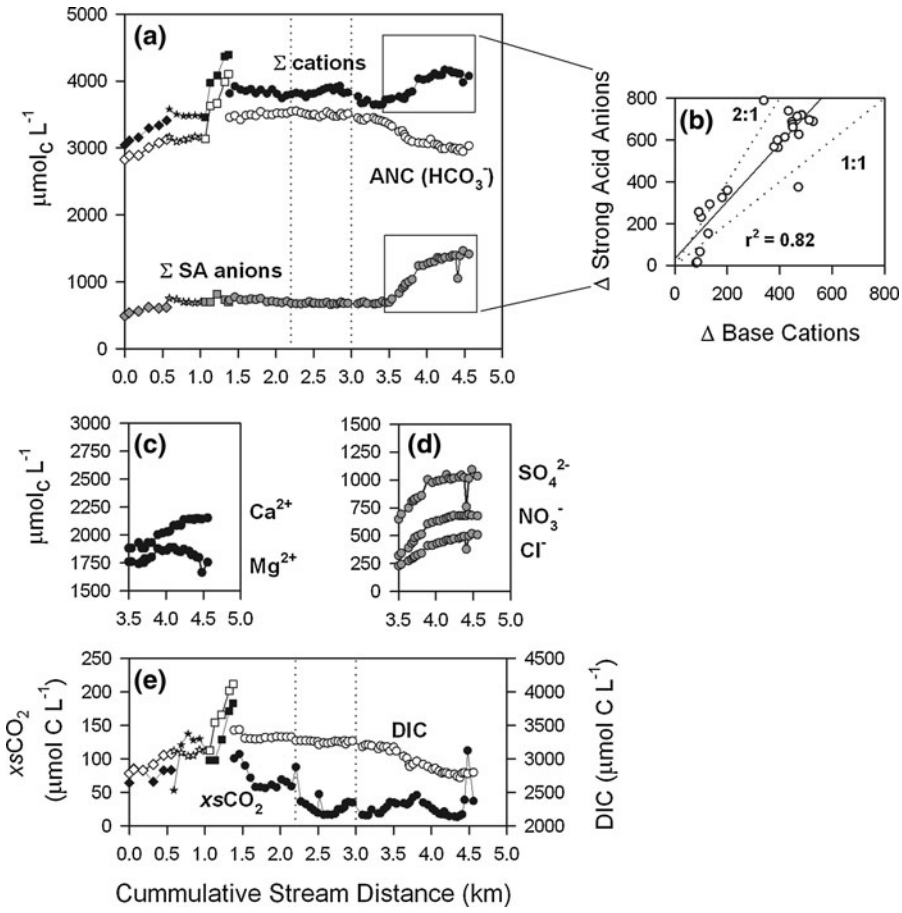


**Fig. 9** Little Plover River surface water chemistry **a** sum of base cations, acid neutralizing capacity, and sum of strong acid anions, **b** correlation between downstream (3.5–4.5 km) stepwise change in base cations and strong acid anions, **c** lower gaining reach calcium and magnesium, **d** lower gaining reach sulfate, nitrate and chloride, and **e** excess carbon dioxide and dissolved inorganic carbon

water quality. First, in the upper drainage network dissolved silica (Si) kept pace with changes in the CFC index; both concentrations of Si and CFC index values exhibit marked decreases with increasing stream distance (Fig. 3e). Second, elevated concentrations of $xsCH_4$ (>0.3 μmol C L$^{-1}$) were highly localized and were restricted to very specific reaches of the LPR (Fig. 3d): (i) in the upper drainage network elevated $CH_4$ concentrations occurred near a stagnant agricultural drainage ditch; and (ii) in the lower drainage network elevated $CH_4$ concentrations coincident with an area of intense ground water seepage and low CFC index values. Third, subtle $xsCO_2$ peaks at several locations along the stream corridor (e.g., 1.3, 2.0, and 3.7 km) elicited a concurrent decrease in both pH and DO (Figs. 3c, 9a). Fourth, the lower drainage network exhibited a rapid increase in both $NO_3^-$ and $xsN_2O$ concentrations peaking at 700 and 0.3 μmol N L$^{-1}$, respectively, and dissolved ions over a course of 500 m (Figs. 3f, 9c–e).

The impact of four decades of N enrichment on elevated dissolved ion concentrations in the lower gaining reach of LPR was clearly evident. The increase in major cations (550 μmol$_c$ L$^{-1}$ increase from losing reach) was dominated by $Ca^{2+}$ and $Mg^{2+}$ which maintained close to 2:1 Ca/Mg molar ratio along the entire stream corridor. The increase in strong acid anions (1000 μmol$_c$ L$^{-1}$ increase from losing reach) was dominated by $NO_3^-$ (300 μmol$_c$ L$^{-1}$), $Cl^-$ (300 μmol$_c$ L$^{-1}$), and $SO_4^{2-}$ (400 μmol$_c$ L$^{-1}$) (Fig. 9). This disproportionate (nearly 2:1) increase in strong acid anions over base cations was responsible for an abrupt decrease in ANC. Field pH measurements showed ANC was comprised almost entirely of $HCO_3^-$ (Figs. 3, 9).

Dissolved gas measurements of several contrasting baseflow-dominated streams revealed significant variation in concentrations over longitudinal distances in all but one stream (Fig. 10). All streams that showed significant longitudinal variability in greenhouse gas concentrations (LPR, BV3, and BV4) were low-order

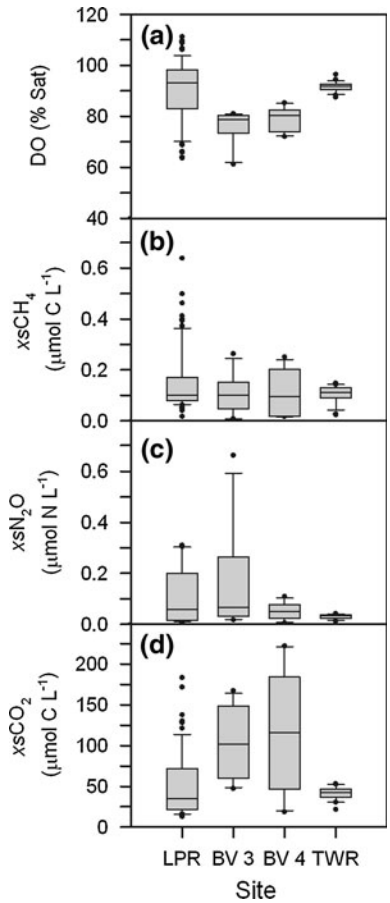


**Fig. 10** Comparison of greenhouse gas concentrations in contrasting central Wisconsin baseflow-dominated steams **a** dissolved oxygen percent saturation, **b** excess methane, **c** excess nitrous oxide, and **d** excess carbon dioxide. Little Plover River (LPR), Buena Vista Ditch #3 (BV 3), Buena Vista Ditch #4 (BV 4), and Tomorrow-Waupaca River (TWR)

(<3) or head water catchments. The fifth-order TWR exhibited very little longitudinal variation in greenhouse gas concentrations (Table 1). Dissolved oxygen was characteristically low in both agricultural drainage ditches (BV 3 and BV 4) and was accompanied by elevated concentrations $CO_2$. The highest concentration of $xsN_2O$ was >0.6 µmol N $L^{-1}$ found in BV 3.

## Discussion

### Ground-surface water chemical interactions

The spatial distribution of nutrients and greenhouse gases in subsurface waters were largely determined by flowpath direction and origin. We found gaseous by-products of nitrification, denitrification, and methanogenesis in all subsurface waters. Both nitrification and denitrification can impart distinct gaseous by-products conventional to the "hole-in-the-pipe" conceptual model of Firestone and Davidson (1989). Under oxic conditions, a direct association between $NO_3^-$ and $N_2O$ is manifested as a small fraction of N is converted to $N_2O$ when $NH_4^+$ is oxidized to $NO_3^-$ during nitrification. Under favorable anoxic conditions (i.e., sufficient supply of labile electron donor to reduce $NO_3^-$ under low or absent $O_2$), the $N_2O$ intermediate is consumed ($2NO_3^- \rightarrow N_2O \rightarrow N_2$) en route to reduction to $N_2$; hence, the endproduct of complete denitrification is simply the accumulation of $N_2$. However, under sub-optimal conditions (e.g., inhibitory presence of $O_2$ or an insufficient supply of labile organic carbon), the association among by-products of denitrification becomes complex and intermediate $N_2O$ species can accumulate. Under these conditions, either an inverse association between $N_2O$ and $NO_3^-$ or a direct association between $N_2O$ and excess $N_2$ may arise.

Shallow horizontal flowpath chemistry (i.e., below the south bank gaining reach riparian zone and both sides of the losing reach stream channel) was highly organized and predictable based on thermodynamic constraints and supplies electron donors and acceptors as found by others (Hedin et al. 1998, Duval and Hill 2007). In the near-stream zone, subsurface waters encountered buried organic matter just below the land surface establishing anoxic zones (i.e., hotspots and hot moments of labile electron donors; McClain et al. 2003) of denitrification and methanogenesis evident by elevated concentrations of DOC (>500 µmol C $L^{-1}$), $xsN_2$, and $xsCH_4$ coupled with very low concentrations of $xsN_2O$ and $NO_3^-$ (Figs. 4, 5). The lack of any significant build up of $xsN_2O$ further suggests denitrification to $N_2$, leaving little or no trace of the $N_2O$ intermediate (Fig. 7). CFC age-date estimates of these ground waters were among the youngest (ca. 2000) of the waters studied. Unexpectedly old ground waters present in the same areas can be explained by a blending of young and old ground water parcels naturally or during the sample collection process and/or microbial degradation of CFCs (Plummer and Busenberg 2000) under low $O_2$ conditions.

The chemistry of vertically up-welling ground water is difficult to explain using a classical ground water redox zonation model. The redox patterns of deep up-welling flowpaths were in sharp contrast to those of shallow horizontal flowpaths. By comparison, elevated excess $N_2$ concentrations in shallow horizontal flowpaths were accompanied by high concentrations of DOC and $CH_4$ with low concentrations of $N_2O$; all indicative of an anoxic environment. However, the relatively oxic up-welling ground waters exhibited very low concentrations of DOC and $CH_4$, yet contained high concentrations of both excess $N_2$ and $N_2O$. The oxic conditions in these up-welling ground waters would generally inhibit denitrification, yet the observed quantities of excess $N_2$ (>250 μmol N $L^{-1}$) indicates the establishment of anoxic conditions suitable for denitrification somewhere along the flowpath en route to the stream.

Several observations suggest that the processes responsible for both the $N_2$ excess and DO depletion in vertically up-welling ground water were most likely completed in the near water table environment before ground water entered the aquifer. Moreover, the redox patterns and excess $N_2$ concentrations in up-welling ground waters are best explained as a blend of two different ground water parcels: oxic ground water (retaining the strong $N_2O$ signature of nitrification) and anoxic ground water (retaining the excess $N_2$ signature of denitrification) upgradient from the stream.

First, evidence of progressive consumption of electron donors along the ground water flowpaths was absent. In contrast to shallow horizontal flowpaths, the concentration of the mobile electron donor (DOC) was apparently too low across the vertical upwelling transect to significantly deplete $O_2$ or produce excess $N_2$. Moreover, contact of drainage water with buried organic matter, with extended residence time, would have increased excess $N_2$ and DO depletion within the aquifer. However, neither the excess $N_2$ ($r^2 = 0.02$) nor the DO depletion ($r^2 = 0.07$) displayed a significant positive correlation with apparent CFC age. In fact, denitrification progression was greatest in younger ground water and positively correlated ($r^2 = 0.28$, $P < 0.0001$) with ground water age (Fig. 8e). This pattern suggests that heterotrophic consumption of electron acceptors (e.g., denitrification) was weak and that locally anoxic features were generally absent deep within the aquifer.

Second, there was a significant positive relationship ($r^2 = 0.31$, $P < 0.0001$) between $xsN_2O$ and $NO_3^-$ but no association was evident ($r^2 = 0.01$, $P = 0.36$) between $xsN_2O$ and $xsN_2$. This direct relationship between $NO_3^-$ and $N_2O$ is indicative that dissolved $N_2O$ was a by-product of soil nitrification under oxic conditions, rather than a by-product of denitrification under marginally anoxic conditions within the aquifer. Given the high DO and lack of available electron donors, the sequential steps of denitrification, $NO_3^- \rightarrow NO_2^- \rightarrow NO \rightarrow N_2O \rightarrow N_2$ (Tiedje 1988) would likely become disrupted upon encounters with anoxic zones within the aquifer thereby eroding the $N_2O/NO_3^-$ relationship. The $N_2O/NO_3^-$ association was significantly stronger in stream water ($r^2 = 0.86$) than gaining ground waters ($r^2 = 0.31$). We attribute this pattern to the close proximity of minipiezometers in conjunction with the large volume of water pumped (inherent in the PIE method), mixing different adjacent ground waters parcels during sample collection. Thus, it does not appear that either $NO_3^-$ or $N_2O$ were utilized as electron acceptors after reaching the deep aquifer except when the flowpath encountered a near surface organic matter rich zone, such as beneath the south bank riparian zone.

From this evidence, we suggest that $NO_3^-$ and $N_2O$ were completely reduced to excess $N_2$ (leaving little or no trace of $N_2O$) in anoxic zones in the near water table environment before seepage into the aquifer. We surmise that oxic ground water parcels laden with $N_2O$ would be largely associated with the agricultural upland recharge areas that dominate the landscape. Accordingly, we anticipate that anoxic ground water parcels laden with excess $N_2$ are associated with focus recharge areas (e.g., wet depressions conducive to denitrification) and organic matter rich environments adjacent to the stream channel (e.g., riparian zones, wetlands). Hence, each flowpath discharging into the LPR would likely have different proportions of oxic and anoxic ground water reflecting the land use and geomorphology inherent to the recharge area.

## Ground water as a source of greenhouse gases

Juxtaposed chemistries of ground water and stream water can sufficiently explain the observed dissolved gas concentrations in LPR surface water (Fig. 6). Concentrations of GHG in ground waters exceeded

stream water concentrations by >200 μmol C $L^{-1}$ for *xs*$CO_2$ and >0.25 μmol N $L^{-1}$ for *xs*$N_2O$; concentrations of *xs*$CH_4$ in ground and stream water were comparable. Stream reaches with the greatest changes in GHG concentrations consistently coincided with changes in the groundwater seepage pattern (Fig. 10). These data suggest that (i) GHG laden ground water discharging into the LPR can more than account for all the dissolved $CO_2$, $N_2O$, and $CH_4$ in the stream surface water and (ii) degassing of GHG occurred as ground water was exposed to the atmosphere at seepage zones along or in the stream channel. Mole $N_2O$-N/$NO_3$–N ratios (mol $mol^{-1}$ × 100) were higher in oxic ground waters (0.080 ± 0.016 mol%) than stream water (0.026 ± 0.004 mol%) suggesting $N_2O$ was lost to atmosphere upon ground water discharge.

Ground waters were routinely more depleted in DO than stream surface water, suggesting other physical (e.g., re-aeration) and biological (e.g., photosynthesis) processes were active in controlling dissolved gas concentrations in LPR surface water. For example in the losing reach, DO was oversaturated (>105%) to a greater degree than can be accounted for temperature-solubility considerations (i.e., cold water at zones of ground water discharge warming downstream). Also in the losing reach, both $CO_2$ and $CH_4$ remained oversaturated, while $N_2O$ was slightly above atmospheric equilibrium. Respiration of organic matter in the water column and sediments could explain the elevated concentrations of $CO_2$ and $CH_4$ across the losing section despite the downward flux of water. Unfortunately, there is no information available on sediment respiration rates for the LPR and how these contributions vary either diurnally or seasonally.

We hypothesize that LPR stream sediments play a limited role in controlling surface water $N_2O$ concentrations (whether by nitrification or denitrification); rather, agriculturally derived oxic ground water is likely the predominant source of $N_2O$. Further evidence can be drawn from differences in the solubility of $N_2O$ and $CH_4$. If concentration differences between $CH_4$ and $N_2O$ in the losing reach were due to strictly physical re-aeration, we would expect $CH_4$ to reach atmospheric equilibration much faster than $N_2O$ which is ~18 times more soluble. Hence, $CH_4$ concentrations should be much lower than observed values in the losing reach due to evasion to the atmosphere. Instead, $CH_4$ remained oversaturated suggesting some amount of methanogenesis and thereby potential $N_2O$ consumption in the stream sediments and/or lateral entry of shallow anoxic soil water (which could be devoid of $N_2O$; i.e., Fig. 5) not captured by the ground water seepage measurements. Ostensibly, the strongest support comes from gaining reaches, where elevated $N_2O$ concentrations only occur when accompanied by large increases in $NO_3^-$ (Fig. 8d).

Neglecting to account for groundwater inputs of GHGs into agricultural streams may lead to (i) large over or under estimates of catchment wide GHG evasion; (ii) overstating GHG production by the water column or sediments; (iii) incomplete understandings of GHG production from non-agricultural landscapes (e.g., riparian zones, wetlands); and (iv) inaccurate predictions on how stream water quality and GHG production will respond to land use changes.

Diurnal variations in $N_2O$ concentrations were not measured but are presumed to be small as the contributions from ground water seepage should be fairly constant given the CFC age dates of the ground waters sampled. However, the $CO_2$ and $O_2$ should exhibit strong diurnal patterns; whether such patterns exist in the LPR remains unknown. We acknowledge our results may reflect time of day biases for some of the water chemistry (e.g., $CO_2$, pH, and $O_2$). Diurnal or seasonal GHG concentrations have been found to be highly variable in some stream ecosystems (Harrison et al. 2005).

## Agricultural acidification and stream water quality

The abrupt increase in major ion concentrations across the lower gaining reach is consistent in part with the theory that carbonate materials were dissolved or cations were displaced from the soil exchange complex (Böhlke and Denver 1995, Bohlke 2002, Denver et al. 2010) by agricultural N acidification via soil nitrification (Eq. 4). The oxidation of $NH_4^+$ consumes acid neutralizing capacity (ANC) in soil solution (carbonate ions) or soil/bedrock solid mineral phases (ion exchange surfaces or carbonate minerals, Eq. 5) to buffer pH. Given sufficient supplies of carbonate minerals (e.g., dolomite) in the soil (natural or amended), the net effect of

nitrification in oxic drainage water should result in a stoichiometric increase in concentrations of $Ca^{2+}$, $Mg^{2+}$, and $HCO_3^-$ in response to increasing concentrations of $NO_3^-$ (Eq. 6).

$$NH_4^+ + 2O_2 = NO_3^- + 2H^+ + H_2O \quad (4)$$

$$CaMg(CO_3)_2(s) + 2H^+ = Ca^{2+} + Mg^{2+} + 2HCO_3^- \quad (5)$$

$$CaMg(CO_3)_2(s) + NH_4^+ + 2O_2 = Ca^{2+} + Mg^{2+} + 2HCO_3^- + NO_3^- + H_2O \quad (6)$$

Other sources of agricultural acidity in addition to soil nitrification appear to contribute to the loss of ANC in the LPR (Fig. 9). Amendments of elemental sulfur can oxidize to produce sulfuric acid (also used to desiccate potato crops prior to harvest). High concentrations of sulfate ($SO_4^{2-}$) were observed in the lower reach of the gaining section coincident with the increasing concentrations of $NO_3^-$ and $Cl^-$. There was a strong correlation ($r^2 = 0.91$, $P < 0.0001$) between $NO_3^-$ and $Cl^-$ which maintained a nearly 1:1 M ratio ($0.89 \pm 0.03$) in stream water. This pattern suggests the major source of $Cl^-$ was derived from nitrogenous compounds, conserved through the nitrification of ammonium chloride ($NH_4Cl$) fertilizer. Other sources of strong acid anions include mineralization and nitrification of organic N in applied animal waste and the dissolution of various salts in fertilizers and animal waste streams. Clearly, agricultural activity impacted the major ion chemistry in the lower gaining reach.

The LPR ground water basin apparently lacks sufficient supplies of cations from carbonate minerals or on the soil exchanger to completely neutralize agricultural acidity (inherent to some sandy outwash plains). This pattern was manifested in the loss of ANC in the lower gaining reach due to a disproportionate (nearly 2:1) increase in strong acid anions over base cations. In a closed ground water, ANC titration by strong acid anions (i.e., $NO_3^-$, $Cl^-$, $SO_4^{2-}$) would increase $CO_2$ acidity, but because this inorganic carbon is not lost from the system; DIC remains conserved. However, upon exposure to the atmosphere, acidified ground waters could degas a substantial portion of $CO_2$ acidity resulting in a loss of DIC and increased pH. Coincident decreases in both DIC and $CO_2$ concentrations in the lower gaining reach supports the hypothesis that agriculturally acidified ground water laden with $CO_2$ acidity (Fig. 3) degassed while other major ions were conserved. Although $N_2O$ increased along this stream reach, stream water $N_2O$ concentrations were still substantially lower than ground water $N_2O$ concentrations.

Agricultural acidity consumed but never exceeded solution ANC as observed from the tail-end perspective of ground water flowpaths. All gaining reach ground and stream waters exhibited ANC $\geq$ 1000 $\mu mol_c\ L^{-1}$. ANC could be made available from one of two sources: (i) blending with ground water sourced non-agricultural landscapes (i.e., no record of agricultural of N acidification at time of recharge); and (ii) alkalinity generated from heterotrophic denitrification. The generation of alkalinity by heterotrophic denitrification was a small source of $HCO_3^-$ to LPR ground waters. Denitrification generated $HCO_3^-$ averaged $10 \pm 5\%$ of the total $HCO_3^-$ concentration across all gaining ground waters; however, in fully denitrified waters this fraction increased to 25%. Denitrification (along with other redox reactions involving $Fe^{3+}$ and $SO_4^{2-}$) should not be totally discounted as important biological mechanisms to increase both $HCO_3^-$ and pH in stream water (Abril and Frankignoulle 2001).

Our ground water samples represent only a small sample of the underlying biogeochemical conditions beneath the LPR. More extensive anoxic zones may have eluded our sampling efforts and most likely exist somewhere along the stream corridor representing additional hotspots for reducing conditions. For example, a zone (3.0–3.75 km) of intense ground water seepage imparted high $CH_4$ and DOC concentrations and very low CFC index values to the stream water (Fig. 3). These changes in stream water chemistry are consistent with anoxic zones adjacent to the LPR stream channel characterized as young, relatively dilute waters low in dissolved solids and DIC but high $CH_4$ and DOC concentrations. The longitudinal increase in stream pH could be explained both as a result of degassed $CO_2$ acidity along with greater contributions of reduced (e.g., denitrified) ground waters of higher pH.

## Conclusions

Our study of the LPR supports the hypothesis that longitudinal surface water patterns of dissolved gases

can reveal physical and chemical changes in the stream-ground water connection in small baseflow-dominated streams. In the LPR, changes in ground water chemistry were abruptly imparted into the stream quality upon the point of discharge into stream. As different flowpaths entered or desisted along the LPR stream corridor, distinct patterns of dissolved gases inherent of specific hydrologic and biogeochemical processes emerged. By exploring the stream-ground water connection in three dimensional space (horizontally and vertically beneath the stream channel, and longitudinally down the stream corridor) we demonstrate:

1. Ground water can be a significant source of greenhouse gases to surface waters draining agricultural landscapes, specifically headwater streams. Changes in the stream-ground water connection can create seemingly erratic patterns in GHG concentrations over short longitudinal distances (order of meters). Scaling up point measurements taken at widely spaced intervals to estimate catchment-wide GHG evasion may result in substantial error when these patterns are not considered.
2. Shallow flowpaths parallel to soil surface beneath the riparian zone were highly anoxic and rich in DOC establishing favorable environments for denitrification and methanogenesis. The spatial distribution of nutrients and greenhouse gases of horizontal subsurface flow were highly organized and predictable based on thermodynamic constraints and supplies electron donors and acceptors. These subsurface waters were not significant sources of $N_2O$; denitrification proceeded to $N_2$ and likely consumed $N_2O$.
3. Deep vertical up-welling flowpaths were oxic and significant sources of $N_2O$ and $NO_3^-$ to the stream. These ground waters are best explained as a blend of two different ground water parcels: oxic ground water (retaining the strong $N_2O$ signature of nitrification) and anoxic ground water (retaining the excess $N_2$ signature of denitrification). It appears that neither $NO_3^-$ nor $N_2O$ were utilized as electron acceptors after reaching the aquifer except when the flowpath encountered anoxic zones near the soil surface. Hence, nitrification was the major source of $N_2O$ with a legacy dating back to the 1960s with $N_2O$ tracking the seepage of $NO_3^-$ into surface waters.
4. Agricultural acidification enhanced the mobilization of major ions predominantly through soil nitrification and sulfur amendments. Carbonate minerals and exchangeable base cations available to agricultural drainage waters in the LPR basin were less than sufficient to neutralize the acid inputs leading to a consumption of ANC in solution; stream water DIC concentrations decreased as a result of degassed $CO_2$ acidity. Stream reaches receiving large quantities of ground water recharged from agricultural landscapes exhibited significant increases in both nutrient ($NO_3^-$) and non-nutrient ($Ca^{2+}$, $Mg^{2+}$, $Cl^-$, $SO_4^{2-}$) solutes.

**Acknowledgments** We thank the spring 2006 University of Wisconsin Stevens Point Water 480 class, Juliane Bowling, Cory Wallschlaeger, and Jeremy Wyss for their help with this study. This work is dedicated to Bryant A. Browne, a great friend and mentor, who oversaw this work and passed away during the writing of this manuscript.

## References

Abril G, Frankignoulle M (2001) Nitrogen-alkalinity interactions in the highly polluted Scheldt basin (Belgium). Water Res 35:844–850

APHA (1995) Methods for the examination of water and wastewater. American Public Health Association, Washington, DC

Beaulieu JJ, Arango CP, Hamilton SK, Tank JL (2008) The production and emission of nitrous oxide from headwater streams in the Midwestern United States. Glob Chang Biol 14:878–894

Böhlke JK (2002) Groundwater recharge and agricultural contamination. Hydrogeol J 10:438–439

Böhlke JK, Denver JM (1995) Combined use of groundwater dating, chemical, and isotopic analyses to resolve the history and fate of nitrate contamination in two agricultural watersheds, Atlantic Coastal Plain, Maryland. Water Resour Res 31:2319–2339

Bowden WB, Bormann FH (1986) Transport and loss of nitrous oxide in soil water after forest clear-cutting. Science 233:867–869

Browne BA (2004) Pumping-induced ebullition: a unified and simplified method for measuring multiple dissolved gases. Environ Sci Technol 38:5729–5736

Browne BA, Guldan NM (2005) Understanding long-term baseflow water quality trends using a synoptic survey of the ground water-surface water interface, Central Wisconsin. J Environ Qual 34:825–835

Browne BA, Kraft GJ, Bowling JM, DeVita WM, Mechenich DJ (2008) Collateral geochemical impacts of agricultural nitrogen enrichment from 1963 to 1985: a Southern Wisconsin ground water depth profile. J Environ Qual 37:1456–1467

Bu X, Warner MJ (1995) Solubility of chlorofluorocarbon 113 in water and seawater. Deep Sea Res Part I Oceanogr Res Pap 42:1151–1161

Bullister J, Weiss R (1988) Determination of $CCl_3F$ and $CCl_2F_2$ in seawater and air. Deep Sea Res Part I Oceanogr Res Pap 35:839–853

Clough TJ, Bertram JE, Sherlock RR, Leonard RL, Nowicki BL (2006) Comparison of measured and EF5-r-derived $N_2O$ fluxes from a spring-fed river. Glob Chang Biol 12:352–363

Cole JJ, Prairie YT, Caraco NF, McDowell WH, Tranvik LJ, Striegl RG, Duarte CM, Kortelainen P, Downing JA, Middelburg JJ, Melack J (2007) Plumbing the global carbon cycle: integrating inland waters into the terrestrial carbon budget. Ecosystems 10:171–184

Cook P, Favreau G, Dighton J, Tickell S (2003) Determining natural groundwater influx to a tropical river using radon, chlorofluorocarbons and ionic environmental tracers. J Hydrol 277:74–88

Dawson JJC, Smith P (2007) Carbon losses from soil and its consequences for land-use management. Sci Total Environ 382:165–190

Dawson JJC, Hope D, Cresser MS, Billett MF (1995) Downstream changes in free carbon-dioxide in an upland catchment from Northeastern Scotland. J Environ Qual 24:699–706

Denver JM, Tesoriero AJ, Barbaro JR (2010) Trends and transformation of nutrients and pesticides in a coastal plain aquifer system, United States. J Environ Qual 39:154–167

Duval TP, Hill AR (2007) Influence of base flow stream bank seepage on riparian zone nitrogen biogeochemistry. Biogeochemistry 85:185–199

Firestone MK, Davidson EA (1989) Microbiological basis of NO and $N_2O$ production and consumption in soil. In: Andreae MO, Schimel DS (eds) Exchange of trace gases between terrestrial ecosystems and the atmosphere (Dahlem workshop reports). John Wiley & Sons, New York, NY, pp 7–21

Fisher SG, Sponseller RA, Heffernan JB (2004) Horizons in stream biogeochemistry: flowpaths to progress. Ecology 85:2369–2379

Gleason RA, Tangen BA, Browne BA, Euliss NH (2009) Greenhouse gas flux from cropland and restored wetlands in the Prairie Pothole Region. Soil Biol Biochem 41:2501–2507

Guldan NM (2004) Relationships between groundwater recharge dates, nitrate levels, and denitrification in a central Wisconsin watershed. Masters Thesis. University of Wisconsin Stevens Point, Stevens Point, WI

Harrison J (2003) Patterns and controls of nitrous oxide emissions from waters draining a subtropical agricultural valley. Global Biogeochemical Cycles 17. doi:10.1029/2002GB001991

Harrison JA, Matson PA, Fendorf SE (2005) Effects of a diel oxygen cycle on nitrogen transformations and greenhouse gas emissions in a eutrophied subtropical stream. Aquatic Sci 67(3):308–315

Heaton T, Vogel JC (1981) "Excess air" in groundwater. J Hydrol 50:201–216

Hedin LO, von Fischer JC, Ostrom NE, Kennedy BP, Brown MG, Robertson GP (1998) Thermodynamic constraints on nitrogen transformations and other biogeochemical processes at soil-stream interfaces. Ecology 79:684–703

Hlaváčová E, Rulík M, Čáp L, Mach V (2006) Greenhouse gas ($CO_2$, $CH_4$, $N_2O$) emissions to the atmosphere from a small lowland stream in Czech Republic. Arch Hydrobiol 165:339–353

Holocher J, Peeters F, Aeschbach-Hertig W, Kinzelbach W, Kipfer R (2003) Kinetic model of gas bubble dissolution in groundwater and its implications for the dissolved gas composition. Environ Sci Technol 37:1337–1343

Jarvie H, Withers P, Hodgkinson R, Bates A, Neal M, Wickham H, Harman S, Armstrong L (2008) Influence of rural land use on streamwater nutrients and their ecological significance. J Hydrol 350:166–186

Kemp MJ, Dodds WK (2001) Spatial and temporal patterns of nitrogen concentrations in pristine and agriculturally-influenced prairie streams. Biogeochemistry 53:125–141

Kling GW, Kipphut GW, Miller MC (1991) Arctic lakes and streams as gas conduits to the atmosphere—implications for tundra carbon budgets. Science 251:298–301

Lohse KA, Brooks PD, McIntosh JC, Meixner T, Huxman TE (2009) Interactions between biogeochemistry and hydrologic systems. Annu Rev Environ Resour 34:65–96

Martin GE, Snow DD, Kim E, Spalding RF (1995) Simultaneous determination of argon and nitrogen. Ground Water 33:781–785

McClain ME, Boyer EW, Dent CL, Gergel SE, Grimm NB, Groffman PM, Hart SC, Harvey JW, Johnston CA, Mayorga E, McDowell WH, Pinay G (2003) Biogeochemical hot spots and hot moments at the interface of terrestrial and aquatic ecosystems. Ecosystems 6:301–312

Modica E, Reilly TE (1997) Patterns and age distribution of ground-water flow to streams. Ground Water 35:523–537

Neill C, Deegan LA, Thomas SM, Haupert CL, Krusche AV, Ballester VM, Victoria RL (2006) Deforestation alters the hydraulic and biogeochemical characteristics of small lowland Amazonian streams. Hydrol Process 20(12):2563–2580

Nevison C (2000) Review of the IPCC methodology for estimating nitrous oxide emissions associated with agricultural leaching and runoff. Chemosphere Glob Change Sci 2:493–500

Plummer LN, Busenberg E (2000) Chloroflurocarbons. In: Cook PG, Herczeg AL (eds) Environmental tracers in subsurface hydrology. Kluwer Academic Publishers, Norwell, MA, pp 441–478

Reay DS, Smith KA, Edwards AC (2003) Nitrous oxide emission from agricultural drainage waters. Glob Change Biol 9:195–203

River Alliance of Wisconsin (2009) Lateral move: the Isherwood's ditch. [Online] Available at http://www.wisconsinrivers.org/documents/newsletter/RA_News_Spring09_Final.pdf. Accessed 30 April 2010. River Alliance of Wisconsin, Madison, WI

Robertson GP, Paul EA, Harwood RR (2000) Greenhouse gases in intensive agriculture: Contributions of individual

gases to the radiative forcing of the atmosphere. Science 289:1922–1925

Sanders IA, Heppell CM, Cotton JA, Wharton G, Hildrew AG, Flowers EJ, Trimmer M (2007) Emission of methane from chalk streams has potential implications for agricultural practices. Freshw Biol 52:1176–1186

Schlesinger WH, Reckhow KH, Bernhardt ES (2006) Global change: the nitrogen cycle and rivers. Water Resour Res 42. doi:10.1029/2005WR004300

Tiedje JM (1988) Ecology of denitrification and dissimilatory nitrate reduction to ammonia. In: Zehnder AJB (ed) Wiley, Chichester, NY, USA, pp 179–244

Vogel J, Talma AS, Heaton T (1981) Gaseous nitrogen as evidence for denitrification in groundwater. J Hydrol 50:191–200

Warner M, Weiss R (1985) Solubilities of chlorofluorocarbons 11 and 12 in water and seawater. Deep Sea Res A 32: 1485–1497

WDNR (1996) Groundwater sampling field manual. PUBL-DG-038 96. [Online] Available at http://dnr.wi.gov/org/water/dwg/gw/pubs/GW-SFM.PDF. Accessed 30 April 2010. Wisconsin Department of Natural Resources, Madison, WI

Weeks EP, Ericson DW, Holt LR (1965) Hydrology of the Little Plover River basin, Portage County, Wisconsin, and the effects of water resources development. Water Supply Paper 1811. USGS, Reston, VA

Wilcock RJ, Sorrell BK (2007) Emissions of greenhouse gases $CH_4$ and $N_2O$ from low-gradient streams in agriculturally developed catchments. Water Air Soil Pollut 188:155–170

Wilhelm E, Battino R, Wilcock RJ (1977) Low-pressure solubility of gases in liquid water. Chem Rev 77:219–262

Winter TC, Harvey JW, Franke OL, Alley WM (1998) Ground water and surface water—a single resource. Circular 1139 [Online] Available at http://water.usgs.gov/pubs/circ/circ1139. Accessed 30 April 2010. USGS, Reston, VA

Woessner WW (2000) Stream and fluvial plain ground water interactions: rescaling hydrogeologic thought. Ground Water 38:423–429